Molecular and Cellular Endocrinology 276 (2007) 24–35

www.elsevier.com/locate/mce

# Characterization of Tusc5, an adipocyte gene co-expressed in peripheral neurons☆

Pieter J. Oort[a], Craig H. Warden[b], Thomas K. Baumann[c], Trina A. Knotts[a], Sean H. Adams[a,d,*]

[a] *USDA/Agricultural Research Service Western Human Nutrition Research Center, University of California, Davis, CA, USA*
[b] *Department of Pediatrics and Section of Neurobiology, Physiology, & Behavior, University of California, Davis, CA, USA*
[c] *Department of Neurological Surgery, Oregon Health & Science University, Portland, USA*
[d] *Department of Nutrition, University of California, Davis, CA, USA*

Received 28 February 2007; accepted 22 June 2007

**Abstract**

Tumor suppressor candidate 5 (Tusc5, also termed brain endothelial cell derived gene-1 or BEC-1), a CD225 domain-containing, cold-repressed gene identified during brown adipose tissue (BAT) transcriptome analyses was found to be robustly-expressed in mouse white adipose tissue (WAT) and BAT, with similarly high expression in human adipocytes. Tusc5 mRNA was markedly increased from trace levels in pre-adipocytes to significant levels in developing 3T3-L1 adipocytes, coincident with several mature adipocyte markers (phosphoenolpyruvate carboxykinase 1, GLUT4, adipsin, leptin). The Tusc5 transcript levels were increased by the peroxisome proliferator activated receptor-γ (PPARγ) agonist GW1929 (1 μg/mL, 18 h) by >10-fold (pre-adipocytes) to ∼1.5-fold (mature adipocytes) versus controls ($p < 0.0001$). Taken together, these results suggest an important role for Tusc5 in maturing adipocytes. Intriguingly, we discovered robust co-expression of the gene in peripheral nerves (primary somatosensory neurons). In light of the marked repression of the gene observed after cold exposure, these findings may point to participation of Tusc5 in shared adipose–nervous system functions linking environmental cues, CNS signals, and WAT–BAT physiology. Characterization of such links is important for clarifying the molecular basis for adipocyte proliferation and could have implications for understanding the biology of metabolic disease-related neuropathies.
Published by Elsevier Ireland Ltd.

*Keywords:* Adipogenesis; Brain endothelial cell derived gene-1 (BEC-1); PPARgamma; Neuropathy; Thermogenesis

## 1. Introduction

The regulation of body weight and energy storage involves cross-talk among many physiological systems which respond to alterations in hormones, tissue metabolites, environmental cues, and nutrients. Experimental systems which display significant metabolic malleability and coincident large shifts in gene expression, protein translation, and metabolite flux are especially helpful in discovering new molecular players involved with this cross-talk, since the signal-to-noise ratio for detection of biochemical and molecular changes is high. For instance, the impressive thermogenic capacity of rodent brown adipose tissue (BAT) may be leveraged to identify metabolically-relevant genes and to reveal new insights into subcellular metabolite pathways which are relevant body-wide. Spiegelman and colleagues identified peroxisome proliferator-activated receptor-γ (PPARγ) co-activator-1 (PGC-1α) as a cold-induced protein in brown adipocytes (Puigserver et al., 1998; Wu et al., 1999), and subsequent work established an important role for this protein in modulating expression of metabolism-related genes in non-BAT tissues including liver and muscle (see Puigserver, 2005). Based on the premise that genes relevant to thermogenesis and metabolism display temperature-sensitive expression changes

☆ This research has been previously presented in part: P. Oort, C. Farber, C. Warden, J.F. Medrano, L. Pennacchio, S. Adams. Characterization of an Obesity Candidate Gene: Unique Co-Expression in Adipocytes and Sensory Nervous System Structures. Obesity 14(9) Supplement: A205 (Abstract 645-P). Annual Mtg. of the North American Assoc. for the Study of Obesity (NAASO), October 2006, Boston, MA, USA.

* Corresponding author at: USDA/ARS Western Human Nutrition Research Center, 430 West Health Sciences Dr., University of California, Davis, CA 95616, USA. Tel.: +1 530 754 4417; fax: +1 530 752 5271.
*E-mail address:* sadams@whnrc.usda.gov (S.H. Adams).

0303-7207/$ – see front matter. Published by Elsevier Ireland Ltd.
doi:10.1016/j.mce.2007.06.005

in BAT, brown fat transcriptomes from mice kept at thermoneutrality (33 °C, 3 week), just below thermoneutrality (22 °C), or maintained in the cold (4 °C, up to 2 days) have been compared (Adams et al., 2001; Yu et al., 2001; Yu et al., 2002). The unique mitochondrial carrier protein CGI-69 (Yu et al., 2001) and a novel acyl-CoA thioesterase (Adams et al., 2001) were among the many differentially-expressed genes induced by cold exposure and whose tissue expression patterns suggested activities beyond brown fat. Furthermore, BAT expression patterns of a large suite of metabolically-important genes – coupled to *in vivo* measures of BAT metabolite flux – revealed that cold elicits a coordinated, paradoxical and energetically futile co-induction of *de novo* lipid synthesis and mitochondrial ß-oxidation in this tissue (Yu et al., 2002). It was thus inferred that distinct subcellular pools of lipogenic versus inhibitory malonyl-CoA exist within brown adipocytes (malonyl-CoA inhibits carnitine palmitoyltransferase-1 and hence ß-oxidation, but also serves as an important lipogenic metabolite)(Yu et al., 2002).

Relatively little is known about warmth-induced or cold-repressed transcripts in BAT or white adipose tissue (WAT). Genes which normally function in "governor" pathways for non-shivering thermogenesis and/or BAT growth are hypothesized to be down-regulated with exposure to cold. Cold-repressed genes might also participate in activities important to temperature-related shifts in macronutrient utilization and storage. Herein, we characterize a cold-repressed transcript discovered in the course of previously-described murine BAT studies (see Adams et al., 2001; Yu et al., 2001; Yu et al., 2002 for animal model details) and initially termed adipose abundant protein (AAP) (WO/2002/097036, Adams 2002). Three splice variants of the human AAP orthologue were cloned from human tissue libraries with transcript lengths of 1.5, 1.9, and 2.7 kb, each containing an identical open reading frame (ORF) encoding a 177 amino acid, 19.1 kDa protein containing two carboxy-terminus transmembrane regions (WO/2002/097036, Adams 2002). The AAP gene has subsequently been termed tumor suppressor candidate 5 (Tusc5) in the public databases (GenBank: NM_177709 and NM_172367 for murine and human sequences, respectively), a nomenclature derived from a report suggesting loss of the gene in certain lung cancer cells (Konishi et al., 2003). Initial studies led to the concept that this gene has a role in regulating BAT and white adipose tissue metabolic function or abundance (WO/2002/097036, Adams 2002): First, tissue expression patterns revealed relatively high Tusc5/AAP mRNA abundance in human WAT and hibernoma (an adipose growth with BAT characteristics) and in the WAT and BAT of mice, with a marked 81% reduction of WAT transcript levels in cold-exposed mice. Second, limited studies in a 3T3-L1 cell culture model indicated that the gene is induced during progression of adipocyte differentiation. Very recently, Shibata et al., identified rat Tusc5 (termed brain endothelial cell derived gene-1, or BEC-1, in their paper) as a gene robustly-expressed in WAT and BAT and, similar to our studies in the mouse, found that the gene was cold-repressed in BAT (Shibata et al., 2007).

The studies herein were designed to further understand the basic biology of Tusc5/BEC-1 and the timecourse of its induction during adipogenesis. To this end, we provide a comprehensive analysis of human and mouse Tusc5 tissue specificity, protein domain analysis, and we detail induction of the gene during the adipocyte differentiation program relative to multiple functional and growth-dependent adipocyte genes. In addition, we evaluated the hypothesis that Tusc5 expression, like several other genes important to adipocyte maturation and function is regulated by PPARγ. Marked Tusc5 mRNA up-regulation in differentiating 3T3-L1 adipocytes in parallel with several late adipogenesis markers and increases in expression following PPARγ agonist treatment are consistent with the idea that Tusc5 plays a role in the physiology of relatively mature adipocytes. The unexpected discovery that Tusc5 is co-expressed in peripheral neurons and WAT highlights a potential shared role for the protein in these systems, with implications for understanding molecular phenomena associated with neuropathies common in obesity and type 2 diabetes.

## 2. Materials and methods

### 2.1. 3T3-L1 adipocyte differentiation and PPARγ agonist studies

Murine 3T3-L1 fibroblasts (ATCC, Manassas, VA) grown to between five and nine passages were induced to differentiate into adipocytes using a protocol similar to Farmer et al. (i.e., Stephens et al., 1999). Briefly, 2-day-confluent cells grown in high-glucose (25 mM) DMEM and 10% FBS (37 °C, 5% $CO_2$) in 6-well rat tail collagen-coated plates were exposed to differentiation medium containing 10 μg/mL bovine insulin (∼1.6 μM), 1 μM dexamethasone, and 0.5 mM 3-isobutyl-1-methylxanthine (IBMX) for 2 days. Cells were grown thereafter in maintenance medium (DMEM/10% FBS + 2.5 μg/mL insulin). Cell culture media was replaced daily. Proof-of-principle studies tested the ability of a single dose of the potent non-thiazoladinedione PPARγ agonist GW1929 (Brown et al., 1999) to stimulate Tusc5 gene expression in non-differentiated confluent 3T3-L1 cells or at various points in the adipocyte differentiation and maturation process as indicated. For these experiments, cells were cultured for the times indicated in media containing vehicle (DMSO; 0.1% by volume) or GW1929 (1 μg/mL, 2.02 μM; 0.1% by volume). At the timepoints indicated, RNA was prepared from 3T3-L1 adipocytes using Trizol-based methods for cell culture samples (Ambion, Austin, TX). RNA abundance and integrity were checked using a NanoDrop® ND-1000 Spectrophotometer (NanoDrop Technologies, Wilmington, DE) and an Agilent 2100 bioanalyzer (Agilent, Foster City, CA) per manufacturer's instructions. Changes in glucose and lactate concentrations in aliquots from the culture media during the adipocyte differentiation timecourse studies (see Section 3) were measured using a YSI 2300 glucose-lactate analyzer (Yellow Springs, OH), and net uptake or output was calculated from metabolite levels pre- and post-treatment.

### 2.2. Gene expression analyses

RNA abundance of Tusc5 and other genes of interest was measured using quantitative real-time PCR. These assays utilized gene-specific TaqMan primers and 5′FAM-3′TAM labeled probes (Assays-on-Demand®, Applied Biosystems Inc., Foster City, CA; see Supplemental Tables 1 and 2) and were run in duplicate or triplicate for each sample using an ABI 7900HT instrument. For tissue panel gene expression patterns, one-step RT-PCR using total RNA as template was used. Human samples were assayed in 30 μL reactions (96-well format) containing: 100 ng RNA, 1× Master Mix (ABI One-Step RT-PCR Master Mix, part #4309169), 1× primer/probe mixture. Cycle conditions were 48 °C 30 min, 95 °C 10 min, then 45 cycles of 95 °C for 15 s/60 °C for 1 min. Mouse tissue panel samples were assayed in 12 μL reactions (384-well format) containing 50 ng RNA and 1× each Master Mix and primer/probe mix. Gene expression for all other studies was analyzed using a two-step process with preparation of cDNA from total RNA, followed by quantitative real-time PCR. Briefly, for each sample, cDNA was prepared from 5 μg of total RNA using Superscript III reverse transcriptase (Invitrogen, Carlsbad, CA) followed by RNAse-H treat-

ment per manufacturer's instructions. Reactions (6 μL/well) were carried out in 384-well format and contained: cDNA corresponding to 50 ng of original total RNA, 1× Master Mix (ABI Universal PCR Master Mix, Part #4304437), 1× primer–probe mix. Cycle conditions were as described above, except without the 48 °C step. Amplification cycle number (Ct) of 18S for each sample was determined using commercial 18S primers and probe (ABI) to correct for template loading differences across all target genes (ΔCt method: ΔCt = sample Ct − 18S Ct). For each gene, individual sample ΔCt values were subtracted from computed average control group ΔCt to derive a sample's ΔΔCt. Since Ct values are not linear with respect to changes in target RNA abundance, the control group computed average ΔCt was calculated using the following formula ($n = 3$ control samples, for illustration):

$$\text{control group computed average } \Delta\text{Ct} = \Delta\text{Ct}_1 - \log_2(\text{AVERAGE}(2^{(\Delta\text{Ct}_1-\Delta\text{Ct}_1)}, 2^{(\Delta\text{Ct}_1-\Delta\text{Ct}_2)}, 2^{(\Delta\text{Ct}_1-\Delta\text{Ct}_3)}))$$

where $\Delta\text{Ct}_1$ is the ΔCt associated with the first control sample, $\Delta\text{Ct}_2$ is the ΔCt associated with the second control sample, and $\Delta\text{Ct}_3$ is the ΔCt associated with the third control sample, and so on (formula is modified for any number of experimental replicates). The Excel spreadsheet formula associated with this calculation (for three control samples, e.g.) is: $\Delta\text{Ct}_1 - \text{LOG}(\text{AVERAGE}(\text{POWER}(2,\Delta\text{Ct}_1-\Delta\text{Ct}_1), \text{POWER}(2,\Delta\text{Ct}_1-\Delta\text{Ct}_2), \text{POWER}(2,\Delta\text{Ct}_1-\Delta\text{Ct}_3)),2)$, where the ΔCt notations are replaced with relevant corresponding spreadsheet cell locations. In mathematical notation:

$$\Delta\text{Ct} = \Delta\text{Ct}_1 - \log_2\left(\frac{\sum_{i=1}^{n}(2^{(\Delta\text{Ct}_1-\Delta\text{Ct}_i)})}{n}\right)$$

where $\Delta\text{Ct}_1$ is the ΔCt associated with the first control sample, $n$ is the number of experimental samples within the control group, and $\Delta\text{Ct}_i$ is the ΔCt associated with each individual sample in sequence within the control group. This approach may also be used for calculating the computed average for analytical replicates within a sample, utilizing raw Ct values within a group instead of ΔCt.

### 2.3. In situ hybridization (ISH) of Tusc5 in murine somatosensory structures (dorsal root ganglia and trigeminal ganglia)

#### 2.3.1. Tissue collection and processing

Animal protocols were approved by the Oregon Health and Science University Institutional Animal Use and Care Committee and followed Animal Welfare Act guidelines. Male C57BL/6J mice aged ~10 months and harboring a neuron-specific yellow fluorescent protein (YFP) transgene (Feng et al., 2000) were housed under standard temperature (20–22 °C) and light/dark cycle (12 h:12 h, lights off at 18:00) conditions and fed rodent chow *ad libitum* (LabDiet 5001, Purina). Mice were killed under $CO_2$, and the lumbar (L4/L5) dorsal root ganglia (DRG) and a trigeminal ganglion (TG) were removed and fixed in 10% formalin (formaldehyde in neutral-buffered sodium phosphate; STATLAB Medical Products, Lewisville, TX) for 24 h. Tissues were transferred to 70% ethanol for storage until processing at the UC Davis Mutant Mouse Pathology Core lab for *in situ* hybridization to determine cell-specific Tusc5 expression. Samples were processed and paraffin embedded using the Sakura Tissue-Tek VIP processor. Four micron sections were prepared with a Leica microtome. Briefly: on Day 1, tissues were deparaffinized in xylene (three changes, 5 min each), followed by two changes each of 100% ethanol (2 min), 95% ethanol (2 min), 70% ethanol (2 min), and PBS (5 min, then held in PBS for 2 h). Samples were treated (37 °C, 15 min) with proteinase K (50 μg/mL in PBS) or PBS (no PK), digestions were stopped with glycine (2 mg/mL glycine in PBS, 15 min), and samples rinsed twice in PBS (5 min each). Slides were then treated with pH 7.0 hybridization buffer with no probe (37 °C, 30 min). On Day 2, Tusc5 sense or antisense probe was added to hybridization solution (2 μL probe/200 μL solution, 5–10 nM probe), denatured (105 °C, 5 min) and placed on ice immediately. Probe solutions were added to slides at 100 μL/slide, slides covered with DNAse–RNAse-free plastic cover slips, and incubated in a humidifying chamber overnight at 37 °C, 15 min. On Day 2, slides were rinsed four times (15 min each, 37 °C) with 0.5× SSC, then four times with 0.2× SSC (15 min each, 37 °C), then allowed to cool to room temperature before incubating 30 min with blocking buffer (Roche DIG Wash and Block Buffer Set, Cat.#11585762001) in a humidifying chamber. Samples were incubated (45 min, 37 °C) with sheep anti-digoxigenin antibody (5 μL to 2.5ml blocking solution; 1:500), washed twice in wash buffer at room temperature, rinsed for 5 min in PBS, and equilibrated in detection buffer for 5 min. The chromogen NBT/BCIP (200 μL:10 mL detection buffer) was added (100 μL/slide, 37 °C), and color development was checked under light microscopy every 30 min. Color development was stopped with water.

#### 2.3.2. Hybridization

Sense (5′ AGG GGG ATG AGG TTG AGG GGC CAG ACG GGG CAG AAG CA 3′) and anti-sense (5′ TGC TTC TGC CCC GTC TGG CCC CTC AAC CTC ATC CCC CT 3′) oligonucleotide probes (spanning nucleotides 693–730 of the NM_177709 murine Tusc5 sequence) were 3′-labeled with digoxigenin (DIG) per manufacturer's instructions (Roche Diagnostics GmgH, Mannheim, Germany, Cat. No. 03353575910). The probe sequence was evaluated for specificity through BLAST analysis (NCBI) and did not match database sequences other than Tusc5.

### 2.4. Materials

Insulin, dexamethasone, IBMX, and GW1929 were purchased from Sigma (St. Louis, MO), DMEM and FBS from Gibco/BRL (Invitrogen, Carlsbad, CA), and cell culture plates were purchased from Nunc (Rochester, NY). Murine and human total RNA tissue panels were obtained from Clontech (Mountain View, CA), with human pre-adipocyte (stromal–vascular cells from WAT biopsy) and cultured and fresh adipocyte total mRNAs bought from Zenbio (Research Triangle Park, NC). A subset of mouse tissue RNAs was prepared from pooled adult C57BL/6J mouse tissues (gonadal fat pad, ear pinna).

### 2.5. Statistics

Comparisons of the effects of the PPARγ agonist GW1929 on gene expression in preadipocytes and adipocytes treated for 7 days were evaluated using a one-way ANOVA, with post hoc Newman-Keuls Multiple Comparison Test (Prism 4.03 software; GraphPad, San Diego, CA). Changes in gene expression over time ± PPARγ activation during 3T3-L1 adipogenesis were evaluated using a two-way ANOVA testing for significant effects of time, treatment, and time × treatment interaction. $p < 0.05$ was considered statistically-significant for all tests. Mean ± S.E.M. are presented.

## 3. Results

### 3.1. Tissue expression profile of Tusc5

Quantitative real-time RT-PCR results from initial studies suggested relatively high expression of the Tusc5 gene in murine WAT and BAT (WO/2002/097036, Adams 2002). We aimed to confirm and extend these findings in mouse and human tissues using analytical and bioinformatic approaches. Consistent with the prior results, we confirmed high WAT Tusc5 expression in the mouse relative to other tissues (Fig. 1A). To address the tissue specificity of Tusc5 across a broader range of tissue types, we evaluated gene chip expression surveys catalogued in SymAtlas, a public database constructed by the Genomics Institute of the Novartis Research Foundation (GNF, San Diego, CA; http://symatlas.gnf.org/SymAtlas/) (Su et al., 2002). In line with the quantitative RT-PCR results, SymAtlas results point to strong Tusc5 expression in BAT and WAT of mice (higher in WAT), with negligible expression in 59 other tissues (Table 1). Interestingly, strong to moderate expression was also apparent in the murine dorsal root ganglia (DRG) and trigeminal ganglia (TG), areas involved in peripheral somatosensory nervous function (sensation of temperature, pain, pressure and touch, e.g.),

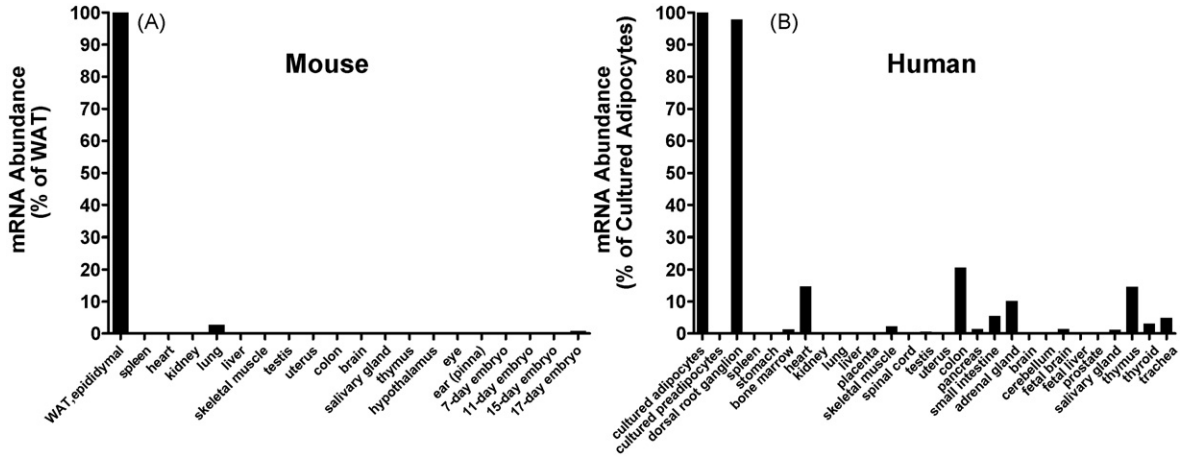


Fig. 1. Tusc5 mRNA profiles in mouse (A) and human (B) Tissues using quantitative real-time RT-PCR reveals robust adipose tissue expression. Tusc5 mRNA abundance in multiple tissues is expressed relative to that observed in WAT (mouse) or cultured adipocytes (human). It was notable that dorsal root ganglia (DRG) of humans displayed robust expression almost equivalent to adipocytes, whereas in cultured human pre-adipocytes no expression was detected.

and in the main olfactory epithelium. In humans, Tusc5 mRNA was found to be most abundant in cultured adipocytes relative to most other tissues queried, with the exception of the DRG which also showed high transcript abundance (Fig. 1B) consistent with the findings in mice (see Table 1, Fig. 1A). As of this writing, no SymAtlas data were available for Tusc5 in humans. Comparing pooled mRNA derived from freshly-isolated purified human adipocytes or subject-matched WAT-derived stromal-vascular non-adipocyte cells ($n = 3$ each), we observed exclusive Tusc5 expression in adipocytes proper (data not shown). There was modest but detectable expression in some non-adipose, non-somatosensory tissues in humans (Fig. 1B), which may signal Tusc5 function at these sites or may simply reflect adipose contamination in the tissues used for preparation of RNA. This issue will need to be resolved in future experiments, but it is notable that a limited study revealed that the commercially-derived human heart sample expressed mRNA for the adipocyte markers leptin, aP2, and PPARγ at ∼5–10% of adipocyte levels (not shown), suggestive of modest fat tissue contamination.

The intriguing co-expression of Tusc5 in adipocytes and peripheral nervous system structures led us to consider whether expression could be traced to peri-neuronal adipocyte-like cells, since the latter have recently been described for sciatic nerves by Lemke et al. (Chrast et al., 2004; Verheijen et al., 2003). However, using the human DRG and cultured human adipocyte mRNAs depicted in Fig. 1, we found trace to no detectable expression of the adipocyte markers leptin, adiponectin, aP2, and PPARγ in DRG, and only modest DRG expression of FAS and GLUT4 (5% and 7% of cultured adipocyte level, respectively), despite the expected robust DRG Tusc5 expression (85% of cultured human adipocyte level in this assay). Follow-on studies using *in situ* hybridization of murine DRG and TG established that Tusc5 expression is confined to the neuronal cell bodies, with no detectable expression in the glial/satellite cell compartment (Fig. 2A–H). In an initial experiment which was confined to the murine TG, we have observed that Tusc5 protein expression is evident in this tissue (Supplemental Fig. 1A). Thus, results to date indicate that Tusc5 displays a unique co-expression in white adipocytes and primary somatosensory neurons.

Table 1
Tusc5 transcript abundance in mouse tissues assayed by gene chip analysis (SymAtlas)

| SymAtlas gene chip public database results (61 tissues) | |
|---|---|
| Murine tissue(s) | Tusc5 expression (arbitrary units) |
| BAT | 1267 |
| WAT | 2634 |
| Dorsal root ganglia (DRG) | 7287 |
| Trigeminal ganglia (TG) | 2656 |
| Main olfactory epithelium | 885 |
| Adrenals | 220 |
| All other tissues | <200 |

Data are from mouse gene chip expression surveys catalogued in SymAtlas, a public database constructed by GNF (http://symatlas.gnf.org/SymAtlas/) (Su et al., 2002). The results are derived from the dataset annotated: "Mouse GeneAtlas GNF1M, gcRMA samples (Tusc5 gnf1m08405_at)".

### 3.2. *Tusc5 domain analysis and homologies*

To help understand the potential functional roles of Tusc5, analyses of conserved regions, domain structures and homologue searches were performed. In humans, rodents, and cattle, Tusc5 is predicted to encode proteins with several regions highly-conserved across species, especially after residue 15 (Fig. 3). Tusc5 belongs to a group of diverse proteins which contain a CD225 interferon inducible transmembrane protein domain (pfam analysis; http://www.sanger.ac.uk/cgi-bin/Pfam/getacc?PF04505), the sequence of which was originally derived from the archetypal interferon-responsive 9–27 protein (Deblandre et al., 1995). A putative Tusc5 homolog, proline-rich transmembrane protein 2 (PRRT2), was identified by pfam and BLAST analyses: human PRRT2 protein is 45% identical/69% conserved when compared against the homologous region (residues 75-176) of the human Tusc5 sequence (not shown).

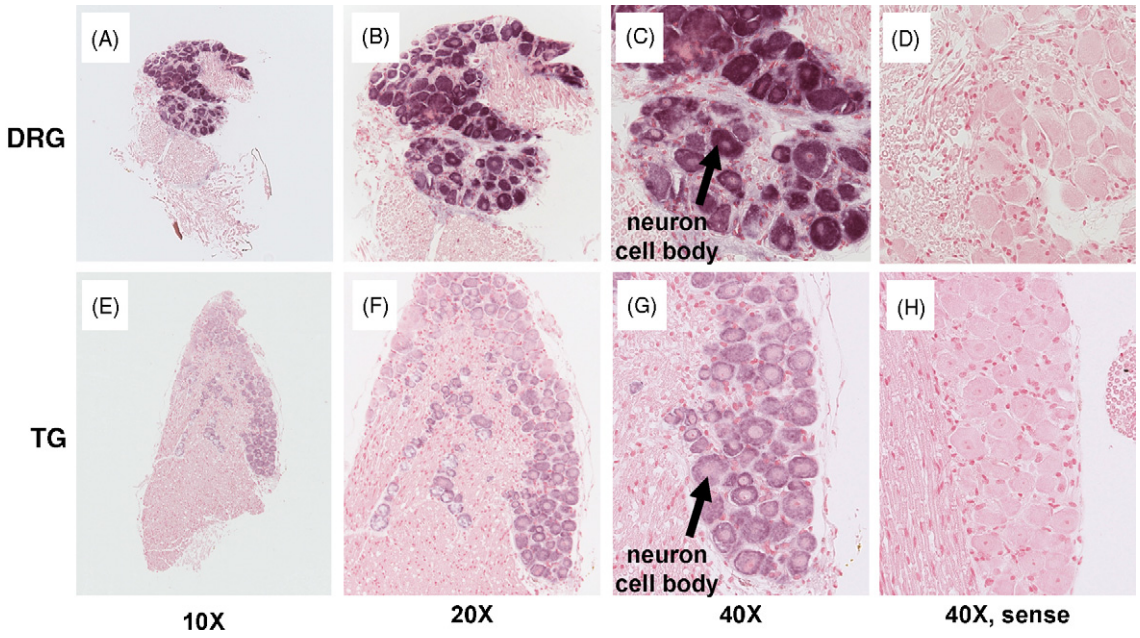


Fig. 2. Neuron-specific expression of Tusc5 in mouse dorsal root ganglia and trigeminal ganglia. Cell-localization of Tusc5 mRNA expression was determined by *in situ* hybridization of DRG and TG cross-sections (see Section 2), and illustrative photographs are depicted at three levels of magnification (photos representative of two independent animals for each ganglion). Purple/dark pink sites are indicative of Tusc5 mRNA expression (Panels A–C; E–G), whereas light pink/white tissue regions indicate hematoxylin/eosin staining only (i.e., Panels D and H, sense probe). The arrows point to the soma of an individual neuron.

```
                          1                                                  50
HUMAN-A          (1)  MAHPVQSEFPSAQEPGSAASLDLPEMEILLTKAENKDDKTLNLSKTLSGP
HUMAN-B          (1)  MAHPVQSEFPSAQEPGSAAFLDLPEMEILLTKAENKDDKTLNLSKTLSGP
CHIMPANZEE       (1)  MAHPVQSEFPSAQEPGSAAPLDLPEMEILLTKAENKDDKTLNLSKALSGP
MOUSE            (1)  MANPAQP--P-LQDPGSTSPLELPEMEKLLTKVENKDDQALNLSKSLSGA
RAT              (1)  MANPVQPQ---LQDPGSTSPLDLPEMEKLLTKVENKDDQALNLSKSLSGA
DOG              (1)  MANPVQPQFPLAQEPGTALPLDLPEMEKLLTKVEGKDDKPLKLSKSLSGA
BOVINE           (1)  MANPGQPQFSAAREPGTASPLNLPEMEKLLVQVGGQDDKSLKPSKSLSGP
                          51                                                 100
HUMAN-A         (51)  LDLEQNGQGLPFKAISEGHLEAPLPRSPSRASSRRASSIATTSYAQDQEA
HUMAN-B         (51)  LDLEQNSQGLPFKAISEGHLEAPLPRSPSRASSRRASSIATTSYAQDQEA
CHIMPANZEE      (51)  LDPEQNGHSLPFKAISEGHLEAPLPRSPSRASSRRVSSIATTSYAQDQEA
MOUSE           (48)  LDLEQNGHSLPFKVISEGHRQPSLSGSPSRVSSRRASSVITTSYAQDQEA
RAT             (48)  LDLEQNGHSLPFKVISEGHRQPSLSGSPSRASSRRASSVVTTSYAQDQEA
DOG             (51)  LDLEQNGHGLPFKVAFEGRQEATLPWSPSRASSRRASSVATASSAQDQEV
BOVINE          (51)  LDLEQNGHSLPFKVISEEHREALHPLSSSRASSRRASSTATTSYAQDGEV
                         101                                                 150
HUMAN-A        (101)  PRDYLILAVVACFCPVWPLNLIPLIISIMSRSSMQQGNVDGARRLGRLAR
HUMAN-B        (101)  PRDYLILAVVACFCPVWPLNLIPLIISIMSRSSMQQGNVDGARRLGRLAR
CHIMPANZEE     (101)  PRDYLILAVVACFCPVWPLNLIPLIISIMSRSSMQQGNMDGARRLGRLAR
MOUSE           (98)  PKDYLVLAIASCFCPVWPLNLIPLIFSIMSRSSVQQGDLDGARRLGRLAR
RAT             (98)  PKDYLVLAIASCFCPVWPLNLIPLIFSIMSRSSVQQGDLDGARRLGRLAR
DOG            (101)  PKDYLILAIASCFCPVWPLNLIPLIFSIMSRSSVQQGDLDGARRLGRLAR
BOVINE         (101)  PKDYLILAIASCFCPVWPLNLMPLIFSIMSRSSVQQGDLDGARRLGRLAG
                         151                 177                 195
HUMAN-A        (151)  LLSITLIIMGIVIIMVAVTVNFTVQKK------------------
HUMAN-B        (151)  LLSITLIIMGIVIIMVAVTVNFTVQKK------------------
CHIMPANZEE     (151)  LLSITLIIMGIVIIMVAVTVNFTVQKK------------------
MOUSE          (148)  LLSITFIILGIVIIIVAVTVNFTVPK-------------------
RAT            (148)  LLSITFIILGIVIIIVAVTVNFTVPK-------------------
DOG            (151)  LLSITFIIMGITIIIVAMTVNFTASFVLWLLITFAMTFLTAKDEY
BOVINE         (151)  TLSITFIIMGITIIIVAVTVNFAVPKK------------------
```

Fig. 3. Amino acid sequence alignment of mammalian tusc5 orthologues. The alignment tool in VectorNTI (Invitrogen) was used to compare known and putative Tusc5 GenBank sequences from two human entries (BAC43751 [HUMAN-A] and NP_758955 [HUMAN-B]), chimpanzees (XP_001153397), mice (NP_808377), rats (NP_001034252), dogs (XP_548306), and cattle (XP_605998). Arrows denote the start and end of a CD225 domain identified in the Tusc5 sequence by pfam analysis.

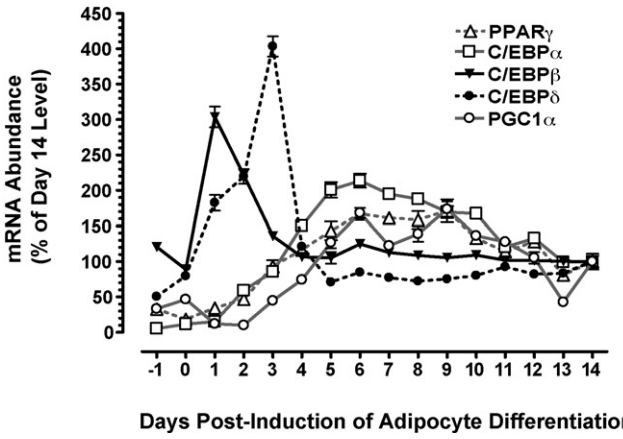


Fig. 4. mRNA expression profile of gene regulatory factors important to 3T3-L1 adipocyte differentiation and maturation. Transcript levels of C/EBPβ, C/EBPδ, PPARγ, C/EBPα, and PGC-1α were determined by quantitative real-time PCR in 3T3-L1 cells at various periods preceding and following initiation of the adipocyte differentiation program (see Supplemental Table 1 for definitions of gene abbreviations). Differentiation of two-day confluent 3T3-L1 fibroblasts was triggered by 48 h exposure of cells to a differentiation medium containing insulin, IBMX, and dexamethasone starting at Day 0, followed by growth in maintenance medium thereafter (see Section 2). Transcript levels for each gene are expressed relative to the mean expression for that gene on Day 14 post-differentiation and expressed as the mean ± S.E.M. of $n = 3$ independent samples/day (note that some error bars are within the symbol; $p < 0.0001$, significant effect of time for each gene).

### 3.3. Gene expression patterns in differentiating 3T3-L1 adipocytes

Determining the time frame over which Tusc5 is expressed during the 3T3-L1 adipocyte differentiation and maturation program (i.e., pre-, early-differentiated to more mature cells) will be helpful to understand when Tusc5 function impacts fat cell physiology. We reasoned that gene regulatory and functional information would emerge from parallel expression analyses of Tusc5, multiple transcription factors, and genes reflecting key adipocyte metabolic roles or differentiation stages (i.e., does Tusc5 cluster with functional gene groups and/or genes with well-characterized gene regulatory elements?). As depicted in Fig. 4, transcription factor expression patterns indicated that our cell culture conditions were optimized to drive expected temporal changes associated with 3T3-L1 adipocyte differentiation: the early genes C/EBPβ and C/EBPδ were triggered in succession and transiently-peaked following initiation of differentiation. Following induction of these genes, factors known to play key roles in driving the full adipocyte phenotype program, PPARγ and C/EBPα, were increased steadily through ∼1 week, with initial induction of the nuclear receptor-regulating protein PGC-1α just following that of PPARγ and C/EBPα.

Tusc5 expression was compared with 21 genes marking differentiation/maturation stages and/or involved in various metabolically-relevant pathways, as derived from the literature. A subjective examination of expression shifts revealed at least six distinct patterns, or gene clusters (Fig. 5). Transcript levels in *Cluster 1* (UCP2 and HDAC3) displayed little change over time from pre-adipocyte to mature adipocyte development, which may be compared to GAPDH (*Cluster 2*) which showed a steady rise starting at ∼3–4 days post-differentiation, reaching a level in mature adipocytes about 2-fold that in pre-adipocytes (Fig. 5A). In contrast, *Cluster 3* genes (resistin, GPDH) were strongly but transiently induced starting at 3 days (Fig. 5A). Transcript abundance for a subset of three genes representing *Cluster 4* (Gata2, Gata3, and KLF6) was reduced significantly immediately following initiation of the differentiation program and remained relatively low versus pre-adipocyte levels throughout the adipocyte maturation process (Fig. 5B). Interestingly, a suite of genes (*Cluster 5*) important to lipid trafficking and fat metabolism (perilipin, HSL, adiponectin, aP2, FAS, glycerol kinase [GlyK], LPL) displayed similar expression patterns which were coincident with PPARγ and C/EBPα transcript shifts (Fig. 5C). In this cluster, mRNA levels increased significantly starting at 2–3 days post-differentiation to amounts ∼1.5–2.5-fold higher versus Day 14 levels by abundance are ∼5 days, remained relatively stable for several days, and decreased from these peak levels starting at ∼9–11 days. Notably, FAS and GlyK patterns differed somewhat from Cluster 5 counterparts in that mRNA level in preadipocytes and early-differentiating adipocytes was roughly equivalent to that in Day 14 adipocytes. Significant induction of Tusc5 expression began at Day 4–5, with peak mRNA abundance noted at Day 9 (Fig. 5D). This pattern of limited to no expression in pre-adipocytes, followed by a marked rise to maximal levels by ∼9 days followed by a modest fall was common among *Cluster 6* genes (Tusc5, PEPCK1, leptin, adipsin, GLUT4). The major induction of Cluster 6 occurred just after Cluster 5 (compare 5C and 5D), also noted in a previous pilot study carried out to 10 days (data not shown). The genes included with Tusc5 in Cluster 6 are considered late/mature adipocyte markers and are known to be responsive to insulin, glucose, glucocorticoids, and/or PPARγ agonists (see Section 4). Note that an unbiased multiscale bootstrap re-sampling analysis essentially concurred with our subjective gene groupings (differences between approaches: bootstrap analysis clustered [GlyK, LPL], [PPARγ, C/EBPα, perilipin, HSL, adiponectin, aP2, FAS], and [resistin, GPDH] as three subgroups of a larger group, and clustered HDAC3 and UCP2 independent from one another).

### 3.4. Effects of the PPARγ agonist GW1929 on expression profiles in 3T3-L1 adipocytes

Many metabolically-relevant adipocyte genes are regulated by PPARγ agonists. Should Tusc5 activity be important to metabolism or adipocyte function, it is reasonable to consider that the Tusc5 gene would be responsive to said agents. In proof-of-principle studies, Tusc5 mRNA was measured in 3T3-L1 pre-adipocytes and adipocytes treated with the potent non-thiazoladinedione GW1929, provided at a concentration just above those reported to stimulate *in vitro* adipocyte glucose uptake and GLUT1 expression (Nugent et al., 2001) and lipogenesis in C3H10T1/2 cells (Brown et al., 1999). Tusc5 expression was strongly induced in both pre-adipocytes and relatively mature adipocytes when grown for 7 days in the presence of GW1929 (Fig. 6): in non-differentiating 3T3-L1 fibroblasts

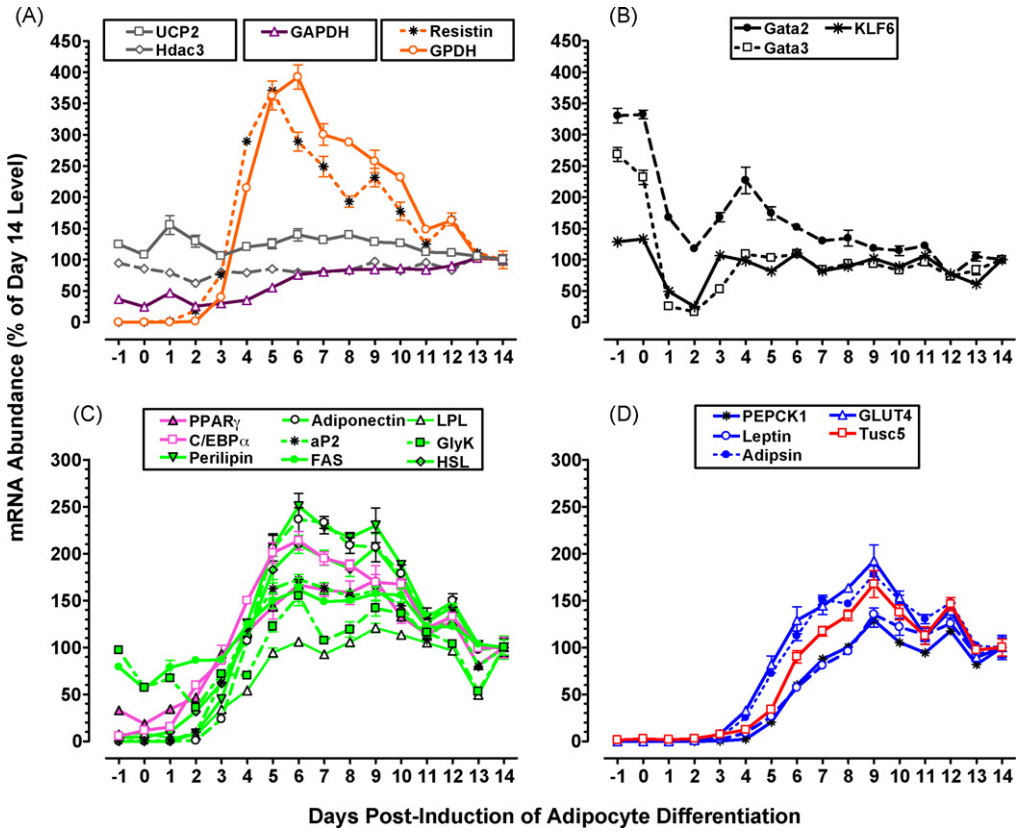


Fig. 5. mRNA expression profile of Tusc5 and a suite of differentiation-stage and functional gene markers in 3T3-L1 adipocytes reveals distinct gene expression clustering patterns. At least six clusters of genes were identified (see boxed legends), each with distinct transcript abundance profile shifts preceding and throughout adipogenesis (see Section 3). mRNA abundance for each gene is expressed relative to the mean level of expression of that gene on Day 14 of differentiation and maturation (see Fig. 4 legend), and symbols represent the mean ± S.E.M. of $n = 3$ samples/day (some error bars are within symbols; $p < 0.0001$, significant effect of time for each gene). Note that profiles of PPARγ and C/EBPα (pink lines, panel C) are the same as those in Fig. 4, and shown here for context. The Tusc5 expression pattern (panel D: red line, open squares) was similar to a cluster containing four other metabolically-relevant genes. See Supplemental Table 1 for definitions of gene abbreviations.

treated with GW1929 for 7 days, the Tusc5 transcript level was equal to that observed in untreated 1 week differentiated adipocytes.

Pilot studies revealed that shorter-term (<24 h) exposure of 3T3-L1 pre-adipocytes and mature adipocytes to 1 μg/mL GW1929 also increased Tusc5 mRNA. To test whether the relative magnitude of this induction changes during adipocyte maturation, and to determine how short-term PPARγ agonist-related Tusc5 expression patterns compare to a large suite of differentiation and functional markers, a group of 3T3-L1 cells were grown 18 h in 1 μg/mL GW1929 in parallel with the untreated cells used for the timecourse studies depicted in Fig. 5. As seen in Fig. 7, treatment of pre-adipocytes or developing fat cells for 18 h with 1 μg/mL GW1929 resulted in distinct gene- and maturation stage-dependent expression patterns. For instance, compared to untreated control cells (considered 100% expression within-day), eight transcripts appeared to be only modestly affected by GW1929 treatment (C/EBPβ, C/EBPδ, FAS, Gata2, Gata3, HDAC3, KLF6), two displayed unique stage-dependent or transient increases (C/EBPα, GAPDH), and one transcript (PPARγ) was unaffected in pre-adipocytes and immature adipocytes, but was significantly and persistently reduced by GW1929 starting at 3–4 days of differentiation (Fig. 7A). Several transcripts were consistently increased by GW1929 treatment but with differing patterns during the adipocyte development process (Fig. 7B): three were increased in pre-adipocytes and at all stages of adipocyte differentiation but with a transiently larger effect in the first days following differentiation (GPDH, PEPCK1, and PGC1α), one was induced by the compound only after initiation of differentiation (GlyK), and one displayed a fairly consistent magnitude of increase at all timepoints (UCP2). Tusc5 and aP2 mRNAs were consistently increased by 18 h GW1929 treatment in pre-adipocytes and at all stages of adipocyte differentiation, but the relative magnitude of this effect was most marked in pre-adipocytes (Fig. 7B). Expression of several genes (adiponectin, GLUT4, HSL, LPL, and perilipin) was activated by GW1929 in pre-adipocytes and newly-differentiated adipocytes, but the compound had little effect on their transcript abundances thereafter – this loss of induction by GW1929 was especially marked for perilipin (Fig. 7C). Finally, transcript levels of three genes (adipsin, leptin, resistin) were increased by GW1929 in pre-adipocytes and immature adipocytes, but decreased by the PPARγ agonist in early-to-late differentiating adipocytes (Fig. 7D). Induction of Tusc5 expression by GW1929 was not associated with changes in net glucose uptake or lactate production in developing 3T3-

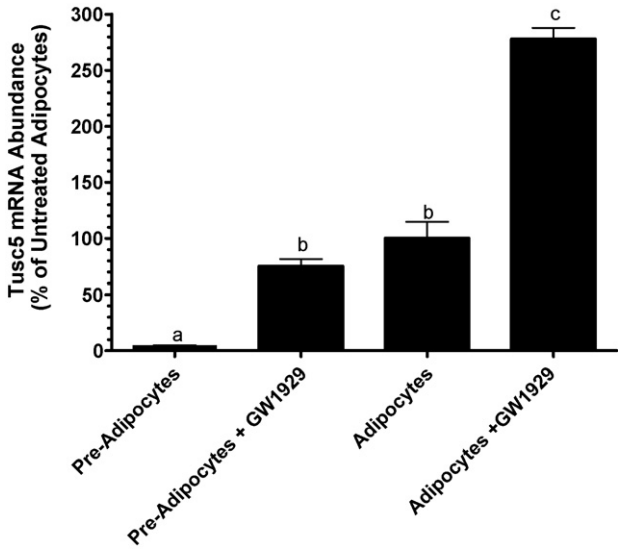


Fig. 6. Increased Tusc5 gene expression following long-term treatment of 3T3-L1 pre-adipocytes and adipocytes with the PPARγ agonist GW1929. 3T3-L1 cells were grown for 7 days with or without GW1929 (1 μg/mL), in basal medium (pre-adipocytes) or under conditions of adipocyte differentiation (see Section 2; $n = 3$/group). Tusc5 mRNA abundance was determined by quantitative real-time PCR, and mean ± S.E.M. are expressed relative to the differentiated adipocytes not treated with compound, considered 100%. Groups which do not share letters display significantly-different Tusc5 expression ($p < 0.001$).

L1 cells, since these parameters did not differ when comparing control versus PPARγ agonist-treated cells (Fig. 8). Our initial studies indicate that Tusc5 protein levels are also increased by GW1929 treatment, and that this effect is long-lasting when the agent is provided during the first two days of differentiation (Supplemental Fig. 1).

## 4. Discussion

Tusc5/BEC-1 is a cold-repressed gene whose robust WAT expression, induction during adipogenesis, and PPARγ agonist responsiveness are consistent with an important role in fat cell physiology. The gene was originally identified using a BAT transcriptome analysis in mice exposed to a range of environmental temperatures (WO/2002/097036, Adams 2002), a strategy which has proven successful in identifying several novel metabolic genes (i.e., BFIT: Adams et al., 2001). Shibata et al. have recently characterized rat Tusc5, describing high levels of WAT and BAT expression and cold-repression in BAT (Shibata et al., 2007), consistent with our findings. Domain analyses and the protein sequence homologies for Tusc5 indicate that the protein is a member of a unique subfamily of CD225-containing proteins implicated in cell cycle regulation and/or modulation of cell proliferation.

One of the most striking and unexpected features of Tusc5 is co-expression in adipocytes and the peripheral nervous system (PNS) somatosensory neurons, which strongly suggests functional cross-talk between these tissues and hence a potential link between environmental cues, the PNS, and adiposity. The potential for interaction between these systems is largely underappreciated, but several examples from the literature suggest that peripheral sensory neurons respond to adipose-derived signals and vice-versa. Fishman and Dark first described somatosensory nervous connections between the DRG and WAT (Fishman and Dark, 1987), but a putative functional role for this circuitry has only recently emerged from the elegant studies of Shi et al. (Shi and Bartness, 2005; Shi et al., 2005). These investigators showed that partial chemical ablation (capsaicin) of the sensory afferents from one distinct WAT depot resulted in expansion of distant depots in rats, thus indicating that modulation of sensory afferent signaling from WAT to the CNS regulates adaptive adiposity changes (also see Bartness et al., 2005). Sensory nerves have been implicated in cold-related brown adipocyte development in WAT depots (Giordano et al., 1998) and they seem to play a role in maintenance of BAT thermogenic responses to norepinephrine (Cui et al., 1990; Osaka et al., 1998). That said, recent studies in which sensory nerve function was reduced by capsaicin injection in WAT do not support a primary role of sensory nerves in WAT proliferation, instead pointing to sympathetic nervous system projections as being key (Foster and Bartness, 2006). Clearly, more research is warranted in this area, especially in light of the fact that WAT sensory ablation is far from complete following local capsaicin treatment (Foster and Bartness, 2006; Shi et al., 2005). Recently, Lemke has described the presence of peri-neuronal (epineurial) adipocytes in studies of peripheral sciatic nerves, along with expression of genes related to lipid accumulation in these cells and in endoneurial/Schwann cells (Chrast et al., 2004; Verheijen et al., 2003), but the implications of this with respect to nervous system function remain unknown. Finally, a number of studies have shown that PNS neurons express adipsin (Cook et al., 1987), adiponectin and leptin receptors, i.e., in vagal afferents (Peters et al., 2004; Peters et al., 2006) and in DRG (Zhou et al., 2005), and respond to adipocyte factors *in vitro* (Turtzo et al., 2001). Future studies will determine if Tusc5 expression is present in additional PNS sites (i.e., nodose neurons, sympathetic neurons), but it is notable that when we mined the NCBI Gene Expression Omnibus gene chip database (http://www.ncbi.nlm.nih.gov/projects/geo/; data deposited by Peeters et al. (2006)), equivalent Tusc5 expression was observed when comparing micro-dissected mouse DRG versus nodose ganglia ($3016 \pm 205.9$ versus $2997 \pm 211.2$ gene chip fluorescence signal units, $n = 9$ and 11, respectively; $p > 0.1$), thus suggesting an important function for the gene in several afferent PNS tissues.

Information gleaned from our comprehensive expression analyses in developing 3T3-L1 adipocytes is consistent with a role for Tusc5 in fat cells near or at maturity, and points to shared gene regulatory elements between Tusc5 and several metabolically-important genes. First, quantitative expression analyses provided a temporal account of transcript changes for adipocyte differentiation and metabolic markers (Fig. 5) and revealed that Tusc5 is strongly induced during the 3T3-L1 adipogenic program concurrent with several genes (PEPCK1, leptin, adipsin, GLUT4) which mark mature differentiated adipocytes (Fu et al., 2005; MacDougald et al., 1995; Tontonoz et al., 1995; Wu et al., 1998). Second, PPARγ is an established regulator of metabolic gene expression and adipocyte maturation, and Tusc5 expression was consistently induced by

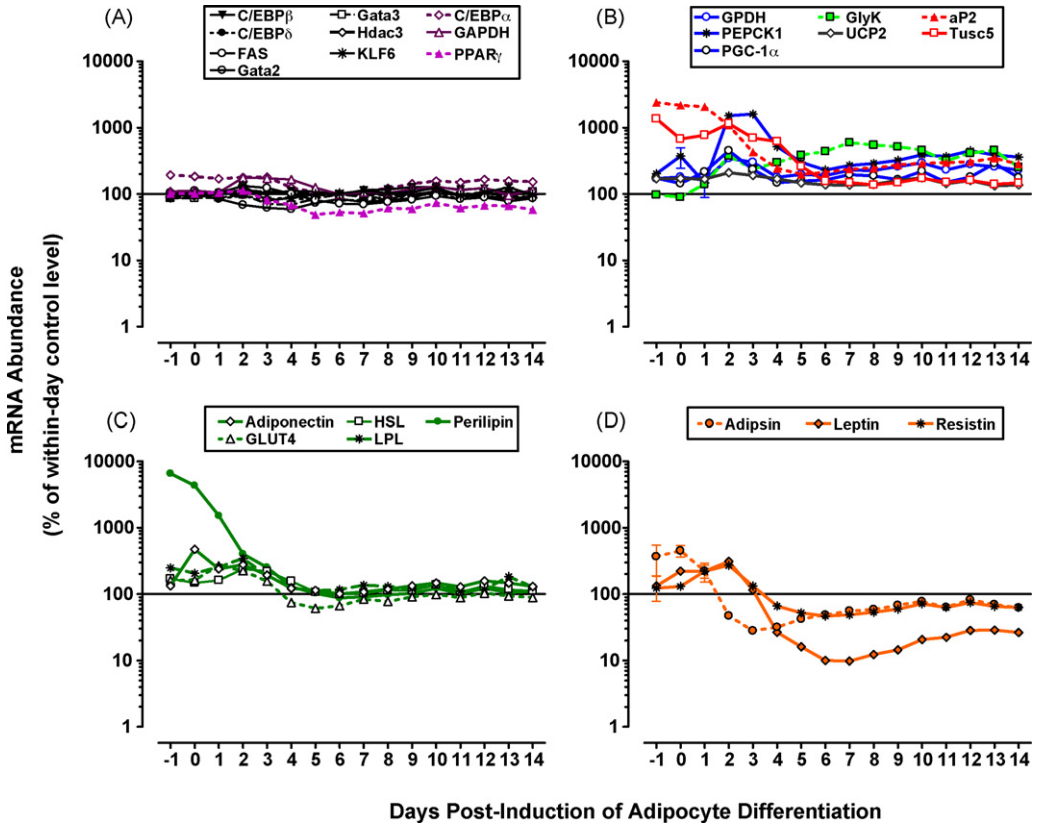


Fig. 7. mRNA expression profile of Tusc5 and a suite of differentiation-stage and functional gene markers in 3T3L1 adipocytes reveals distinct gene expression patterns in response to short-term treatment with the PPARγ agonist GW1929. RNA from undifferentiated 3T3-L1 fibroblasts, differentiating, and maturing 3T3-L1 adipocytes was isolated from cells exposed to GW1929 (1 μg/mL, 18 h; $n = 3$/timepoint), and relative transcript abundances were measured by quantitative real-time PCR for 26 genes including Tusc5. As an example, for Day +1 data, GW1929 was added 18 h prior to cell harvest (GW1929 added on differentiation Day 0 with RNA extraction on Day +1, and so on). Within-day expression of each gene in untreated control cells (see Figs. 4 and 5) was considered 100%, as illustrated by the horizontal line – thus, for each gene values above the line represent induction, whereas values below the line represent repression of transcript abundance relative to that observed in untreated control cells from the same day. Large differences in relative induction or repression of expression by GW1929 were noted across genes; thus, data are presented on a logarithmic scale to enable presentation. Note that Tusc5 expression was induced significantly by GW1929 at all stages of 3T3-L1 development (panel B: red line, open square; see Section 3 for more detail). See Supplemental Table 1 for definitions of gene abbreviations. There was a significant treatment effect ($p \leq 0.001$) and timepoint × treatment interaction ($p \leq 0.001$) for every gene tested except HDAC3 and KLF6 ($p = 0.47$ and $p = 0.35$, respectively, treatment effect). Data are mean ± S.E.M.; some error bars are within symbols.

treatment with the PPARγ agonist GW1929 (see Figs. 6 and 7). PPARγ agonists have been shown to increase gene expression for PEPCK1 (Fu et al., 2005; Glorian et al., 1998) and to decrease leptin expression (Kallen and Lazar, 1996; Murata et al., 2000; Sinha et al., 1999) in mature adipocytes, in line with our results. The effects of these agents on normal fat cell adipsin and GLUT4 appear less clear-cut, but the results of Fu et al. (Fu et al., 2005) and our results (Fig. 7) suggest a repressive influence of PPARγ

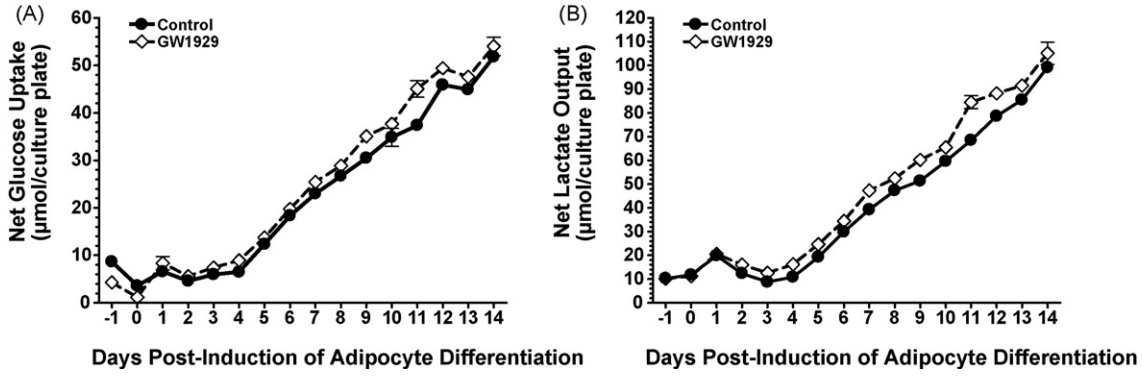


Fig. 8. Differences in net glucose uptake (A) and net lactate output (B) following short-term treatment of 3T3-L1 pre-adipocytes and adipocytes with the PPARγ agonist GW1929. 3T3-L1 cells were grown for 18 h with or without GW1929 (1 μg/mL), in basal medium (pre-adipocytes) or under conditions of adipocyte differentiation (see Section 2; $n = 3$/timepoint/treatment. Note that samples were derived from the same studies depicted in Figs. 5 and 7).

agonists on adipsin expression, whereas GLUT4 is generally reported to be increased with longer-term (≥48 h) exposure to these agents (Tamori et al., 2002; Wu et al., 1998). We noted only modest differences in net glucose uptake and lactate output in 3T3-L1 adipocytes treated 18 h with GW1929 (Fig. 8), similar to others who have reported no effect of short-term rosiglitazone-treatment on glucose uptake in this model (Nugent et al., 2001), and implying that Tusc5 induction following acute GW1929 was not a secondary effect related to changes in glucose utilization. Further studies are required to evaluate whether PPARγ-interacting sites exist in the Tusc5 promoter region and to utilize additional PPARγ agonists to confirm that Tusc5 gene induction is not GW1929-specific and is not due to off-target effects. Since insulin, glucose, glucocorticoids, and some fatty acids influence expression of the genes whose transcript levels clustered with Tusc5 during adipogenesis – PEPCK1 (Antras-Ferry et al., 1995; Chakravarty et al., 2005; Dani et al., 1986; Glorian et al., 1998), leptin (Mueller et al., 1998; Murata et al., 2000; Russell et al., 1998; Wabitsch et al., 1996), adipsin (Dani et al., 1989; Lowell and Flier, 1990; Moustaid et al., 1990), and GLUT4 (Cooke and Lane, 1998; Flores-Riveros et al., 1993; Long and Pekala, 1996) – it will be of interest to test whether these factors also regulate the Tusc5 gene. Finally, it will be important to determine if activation of adipocyte ß3-adrenergic receptors decreases Tusc5 expression, since the gene is repressed by cold in BAT and WAT of mice (WO/2002/097036, Adams 2002) and in BAT of rats (Shibata et al., 2007), a situation in which sympathetic tone to the tissues is activated (Garofalo et al., 1996).

Based on several lines of reasoning, we propose a working model in which Tusc5 participates in "governor" pathways modulating brown or white adipocyte proliferation and/or maintenance of cell cycle growth arrest in response to environmental or CNS cues. First, Tusc5 contains a CD225 interferon (IFN)-induced transmembrane protein domain, originally identified in the archetypal interferon-responsive 9–27 protein which has been implicated in the anti-proliferative actions of IFNs (Deblandre et al., 1995) and is proposed to contribute to cell adhesion properties in lymphocytes and some other cell types (Martensen and Justesen, 2004). There is some suggestion that 9–27 and the related 1–8 proteins are part of a cell-surface family which form multimeric complexes to transduce anti-proliferative and cell adhesion signals via cell–cell interactions (Deblandre et al., 1995; Martensen and Justesen, 2004; Pru et al., 2001). Second, Konishi et al. focused on human Chromosome 17p13.3 as a "hotspot" for deletions in certain cancers (Konishi et al., 2003). Using BAC/YAC clones, genomic bioinformatics, and other molecular approaches, these researchers identified a homozygous deletion in several lung cancer cell lines which included the genes CRK, 14-3-3ε, and Tusc5 (termed LOST1 in their paper). The authors hypothesized that a loss of function due to a breakpoint in the LOST1/Tusc5 Exon 1 – as seen in certain lung cancer lines – could de-repress cancer growth thereby making this gene a tumor suppressor candidate (Konishi et al., 2003). Third, induction of Tusc5 expression is coincident with mature 3T3-L1 adipocyte markers which are known to increase as adipocytes exit the mitotic clonal expansion phase and enter growth arrest/terminal differentiation (Morrison and Farmer, 1999). Fourth, white and brown adipocyte proliferation are expected to be increased and decreased, respectively, in Zucker obese animals and, intriguingly, Tusc5 expression was markedly reduced in WAT and significantly increased in Zucker BAT (Shibata et al., 2007). Thus, results to date are consistent with a potential regulatory role for Tusc5 in tissue growth or cell proliferation, a concept currently under study by our group.

It is tempting to consider that the cold-repression of Tusc5 in rodent BAT and WAT (WO/2002/097036, Adams 2002; Shibata et al., 2007) is an adaptive phenomenon which poises the animal for brown and white adipose malleability (i.e., to increase thermogenesis through brown adipocyte expansion, or to support increased white adipocyte numbers and hence energy storage capacity). The discovery of Tusc5 as a temperature-sensitive, PPARγ agonist-responsive adipocyte gene co-expressed in peripheral neurons may provide a molecular link between environmental cues, adipose tissue status, and energy homeostasis, but further research is needed to understand this putative link and the role of Tusc5 in neurons. Further characterization of Tusc5 may thus have important implications for understanding the physiology of adipogenesis *in vivo*, and may have implications in understanding the etiology and pathophysiology of neuropathies commonly-observed in obesity and type 2 diabetes.

## Acknowledgements

The authors thank Lisa Dillard-Telm and Robert Munn (UCD Mutant Mouse Pathology Lab) for performing *in situ* hybridization studies and generating tissue photos, respectively, Catherine Chamberlain (OHSU) for collection of mouse sensory ganglia tissues, and Anthony Thomas and Lana Lee for analysis of glucose and lactate. We are indebted to Dr. Peter J. Havel (UCD Dept. of Nutrition) for the use of his laboratory's glucose-lactate analyzer, and to Drs. Kyoungmi Kim and Mark Rosenblatt (UCD School of Medicine) for bootstrap analysis of gene expression clusters and mouse trigeminal ganglia tissue, respectively. Work was funded in part by the following: American Diabetes Association Research Grant 7-05RA-07 (T.K.B.), NIH grant DK52581 (C.H.W.), intramural USDA-ARS CRIS 5306-51530-016-00D (S.H.A.), and a USDA Postdoctoral Fellowship to Trina Knotts.

## Appendix A. Supplementary data

Supplementary data associated with this article can be found, in the online version, at doi:10.1016/j.mce.2007.06.005.

## References

Adams, S.H., Chui, C., Schilbach, S.L., Yu, X.X., Goddard, A.D., Grimaldi, J.C., Lee, J., Dowd, P., Colman, S., Lewin, D.A., 2001. BFIT, a unique acyl-CoA thioesterase induced in thermogenic brown adipose tissue: cloning, organization of the human gene and assessment of a potential link to obesity. Biochem. J. 360, 135–142.

Antras-Ferry, J., Robin, P., Robin, D., Forest, C., 1995. Fatty acids and fibrates are potent inducers of transcription of the phosphenolpyruvate carboxykinase gene in adipocytes. Eur. J. Biochem. 234, 390–396.

Bartness, T.J., Kay Song, C., Shi, H., Bowers, R.R., Foster, M.T., 2005. Brain-adipose tissue cross talk. Proc. Nutr. Soc. 64, 53–64.

Brown, A.M., Dolan, J.W., Willi, S.M., Garvey, W.T., Argyropoulos, G., 1999. Endogenous mutations in human uncoupling protein 3 alter its functional properties. FEBS Lett. 464, 189–193.

Chakravarty, K., Cassuto, H., Reshef, L., Hanson, R.W., 2005. Factors that control the tissue-specific transcription of the gene for phosphoenolpyruvate carboxykinase-C. Crit. Rev. Biochem. Mol. Biol. 40, 129–154.

Chrast, R., Verheijen, M.H., Lemke, G., 2004. Complement factors in adult peripheral nerve: a potential role in energy metabolism. Neurochem. Int. 45, 353–359.

Cook, K.S., Min, H.Y., Johnson, D., Chaplinsky, R.J., Flier, J.S., Hunt, C.R., Spiegelman, B.M., 1987. Adipsin: a circulating serine protease homolog secreted by adipose tissue and sciatic nerve. Science 237, 402–405.

Cooke, D.W., Lane, M.D., 1998. A sequence element in the GLUT4 gene that mediates repression by insulin. J. Biol. Chem. 273, 6210–6217.

Cui, J., Zaror-Behrens, G., Himms-Hagen, J., 1990. Capsaicin desensitization induces atrophy of brown adipose tissue in rats. Am. J. Physiol. 259, R324–R332.

Dani, C., Bertrand, B., Bardon, S., Doglio, A., Amri, E., Grimaldi, P., 1989. Regulation of gene expression by insulin in adipose cells: opposite effects on adipsin and glycerophosphate dehydrogenase genes. Mol. Cell. Endocrinol. 63, 199–208.

Dani, C., Doglio, A., Grimaldi, P., Ailhaud, G., 1986. Expression of the phosphoenolpyruvate carboxykinase gene and its insulin regulation during differentiation of preadipose cell lines. Biochem. Biophys. Res. Commun. 138, 468–475.

Deblandre, G.A., Marinx, O.P., Evans, S.S., Majjaj, S., Leo, O., Caput, D., Huez, G.A., Wathelet, M.G., 1995. Expression cloning of an interferon-inducible 17-kDa membrane protein implicated in the control of cell growth. J. Biol. Chem. 270, 23860–23866.

Feng, G., Mellor, R.H., Bernstein, M., Keller-Peck, C., Nguyen, Q.T., Wallace, M., Nerbonne, J.M., Lichtman, J.W., Sanes, J.R., 2000. Imaging neuronal subsets in transgenic mice expressing multiple spectral variants of GFP. Neuron 28, 41–51.

Fishman, R.B., Dark, J., 1987. Sensory innervation of white adipose tissue. Am. J. Physiol. 253, R942–R944.

Flores-Riveros, J.R., McLenithan, J.C., Ezaki, O., Lane, M.D., 1993. Insulin down-regulates expression of the insulin-responsive glucose transporter (GLUT4) gene: effects on transcription and mRNA turnover. Proc. Natl. Acad. Sci. U.S.A. 90, 512–516.

Foster, M.T., Bartness, T.J., 2006. Sympathetic but not sensory denervation stimulates white adipocyte proliferation. Am. J. Physiol. Regul. Integr. Comp. Physiol. 291, R1630–R1637.

Fu, M., Sun, T., Bookout, A.L., Downes, M., Yu, R.T., Evans, R.M., Mangelsdorf, D.J., 2005. A nuclear receptor atlas: 3T3-L1 adipogenesis. Mol. Endocrinol. 19, 2437–2450.

Garofalo, M.A., Kettelhut, I.C., Roselino, J.E., Migliorini, R.H., 1996. Effect of acute cold exposure on norepinephrine turnover rates in rat white adipose tissue. J. Auton. Nerv. Syst. 60, 206–208.

Giordano, A., Morroni, M., Carle, F., Gesuita, R., Marchesi, G.F., Cinti, S., 1998. Sensory nerves affect the recruitment and differentiation of rat perivovarian brown adipocytes during cold acclimation. J. Cell Sci. 111 (Pt 17), 2587–2594.

Glorian, M., Franckhauser-Vogel, S., Robin, D., Robin, P., Forest, C., 1998. Glucocorticoids repress induction by thiazolidinediones, fibrates, and fatty acids of phosphoenolpyruvate carboxykinase gene expression in adipocytes. J. Cell. Biochem. 68, 298–308.

Kallen, C.B., Lazar, M.A., 1996. Antidiabetic thiazolidinediones inhibit leptin (ob) gene expression in 3T3-L1 adipocytes. Proc. Natl. Acad. Sci. U.S.A. 93, 5793–5796.

Konishi, H., Sugiyama, M., Mizuno, K., Saito, H., Yatabe, Y., Takahashi, T., Osada, H., Takahashi, T., 2003. Detailed characterization of a homozygously deleted region corresponding to a candidate tumor suppressor locus at distal 17p13.3 in human lung cancer. Oncogene 22, 1892–1905.

Long, S.D., Pekala, P.H., 1996. Regulation of GLUT4 gene expression by arachidonic acid. Evidence for multiple pathways, one of which requires oxidation to prostaglandin E2. J. Biol. Chem. 271, 1138–1144.

Lowell, B.B., Flier, J.S., 1990. Differentiation dependent biphasic regulation of adipsin gene expression by insulin and insulin-like growth factor-1 in 3T3-F442A adipocytes. Endocrinology 127, 2898–2906.

MacDougald, O.A., Hwang, C.S., Fan, H., Lane, M.D., 1995. Regulated expression of the obese gene product (leptin) in white adipose tissue and 3T3-L1 adipocytes. Proc. Natl. Acad. Sci. U.S.A. 92, 9034–9037.

Martensen, P.M., Justesen, J., 2004. Small ISGs coming forward. J. Interferon Cytokine Res. 24, 1–19.

Morrison, R.F., Farmer, S.R., 1999. Role of PPARgamma in regulating a cascade expression of cyclin-dependent kinase inhibitors, p18(INK4c) and p21(Waf1/Cip1), during adipogenesis. J. Biol. Chem. 274, 17088–17097.

Moustaid, N., Lasnier, F., Hainque, B., Quignard-Boulange, A., Pairault, J., 1990. Analysis of gene expression during adipogenesis in 3T3-F442A preadipocytes: insulin and dexamethasone control. J. Cell. Biochem. 42, 243–254.

Mueller, W.M., Gregoire, F.M., Stanhope, K.L., Mobbs, C.V., Mizuno, T.M., Warden, C.H., Stern, J.S., Havel, P.J., 1998. Evidence that glucose metabolism regulates leptin secretion from cultured rat adipocytes. Endocrinology 139, 551–558.

Murata, M., Kaji, H., Takahashi, Y., Iida, K., Mizuno, I., Okimura, Y., Abe, H., Chihara, K., 2000. Stimulation by eicosapentaenoic acids of leptin mRNA expression and its secretion in mouse 3T3-L1 adipocytes in vitro. Biochem. Biophys. Res. Commun. 270, 343–348.

Nugent, C., Prins, J.B., Whitehead, J.P., Savage, D., Wentworth, J.M., Chatterjee, V.K., O'Rahilly, S., 2001. Potentiation of glucose uptake in 3T3-L1 adipocytes by PPAR gamma agonists is maintained in cells expressing a PPAR gamma dominant-negative mutant: evidence for selectivity in the downstream responses to PPAR gamma activation. Mol. Endocrinol. 15, 1729–1738.

Osaka, T., Kobayashi, A., Namba, Y., Ezaki, O., Inoue, S., Kimura, S., Lee, T.H., 1998. Temperature- and capsaicin-sensitive nerve fibers in brown adipose tissue attenuate thermogenesis in the rat. Pflugers Arch. 437, 36–42.

Peeters, P.J., Aerssens, J., de Hoogt, R., Stanisz, A., Gohlmann, H.W., Hillsley, K., Meulemans, A., Grundy, D., Stead, R.H., Coulie, B., 2006. Molecular profiling of murine sensory neurons in the nodose and dorsal root ganglia labeled from the peritoneal cavity. Physiol. Genomics 24, 252–263.

Peters, J.H., Karpiel, A.B., Ritter, R.C., Simasko, S.M., 2004. Cooperative activation of cultured vagal afferent neurons by leptin and cholecystokinin. Endocrinology 145, 3652–3657.

Peters, J.H., Ritter, R.C., Simasko, S.M., 2006. Leptin and CCK modulate complementary background conductances to depolarize cultured nodose neurons. Am. J. Physiol. Cell Physiol. 290, C427–C432.

Pru, J.K., Austin, K.J., Haas, A.L., Hansen, T.R., 2001. Pregnancy and interferon-tau upregulate gene expression of members of the 1-8 family in the bovine uterus. Biol. Reprod. 65, 1471–1480.

Puigserver, P., 2005. Tissue-specific regulation of metabolic pathways through the transcriptional coactivator PGC1-alpha. Int. J. Obes. (Lond) 29 (Suppl. 1), S5–S9.

Puigserver, P., Wu, Z., Park, C.W., Graves, R., Wright, M., Spiegelman, B.M., 1998. A cold-inducible coactivator of nuclear receptors linked to adaptive thermogenesis. Cell 92, 829–839.

Russell, C.D., Petersen, R.N., Rao, S.P., Ricci, M.R., Prasad, A., Zhang, Y., Brolin, R.E., Fried, S.K., 1998. Leptin expression in adipose tissue from obese humans: depot-specific regulation by insulin and dexamethasone. Am. J. Physiol. 275, E507–E515.

Shi, H., Bartness, T.J., 2005. White adipose tissue sensory nerve denervation mimics lipectomy-induced compensatory increases in adiposity. Am. J. Physiol. Regul. Integr. Comp. Physiol. 289, R514–R520.

Shi, H., Song, C.K., Giordano, A., Cinti, S., Bartness, T.J., 2005. Sensory or sympathetic white adipose tissue denervation differentially affects depot growth and cellularity. Am. J. Physiol. Regul. Integr. Comp. Physiol. 288, R1028–R1037.

Shibata, T., Koide, H., Hayashi, R., Nagata, K., Takeo, C., Yoshida, T., Noguchi, Y., Tanaka, T., Saito, Y., Tatsuno, I., 2007. Molecular cloning and characterization of rat brain endothelial cell derived gene-1 (tumor suppressor candidate 5) expressing abundantly in adipose tissues. Mol. Cell. Endocrinol. 263, 38–45.

Sinha, D., Addya, S., Murer, E., Boden, G., 1999. 15-Deoxy-delta(12,14) prostaglandin J2: a putative endogenous promoter of adipogenesis suppresses the ob gene. Metabolism 48, 786–791.

Stephens, J.M., Morrison, R.F., Wu, Z., Farmer, S.R., 1999. PPARgamma ligand-dependent induction of STAT1, STAT5A, and STAT5B during adipogenesis. Biochem. Biophys. Res. Commun. 262, 216–222.

Su, A.I., Cooke, M.P., Ching, K.A., Hakak, Y., Walker, J.R., Wiltshire, T., Orth, A.P., Vega, R.G., Sapinoso, L.M., Moqrich, A., Patapoutian, A., Hampton, G.M., Schultz, P.G., Hogenesch, J.B., 2002. Large-scale analysis of the human and mouse transcriptomes. Proc. Natl. Acad. Sci. U.S.A. 99, 4465–4470.

Tamori, Y., Masugi, J., Nishino, N., Kasuga, M., 2002. Role of peroxisome proliferator-activated receptor-gamma in maintenance of the characteristics of mature 3T3-L1 adipocytes. Diabetes 51, 2045–2055.

Tontonoz, P., Hu, E., Devine, J., Beale, E.G., Spiegelman, B.M., 1995. PPAR gamma 2 regulates adipose expression of the phosphoenolpyruvate carboxykinase gene. Mol. Cell. Biol. 15, 351–357.

Turtzo, L.C., Marx, R., Lane, M.D., 2001. Cross-talk between sympathetic neurons and adipocytes in coculture. Proc. Natl. Acad. Sci. U.S.A. 98, 12385–12390.

Verheijen, M.H., Chrast, R., Burrola, P., Lemke, G., 2003. Local regulation of fat metabolism in peripheral nerves. Genes Dev. 17, 2450–2464.

Wabitsch, M., Jensen, P.B., Blum, W.F., Christoffersen, C.T., Englaro, P., Heinze, E., Rascher, W., Teller, W., Tornqvist, H., Hauner, H., 1996. Insulin and cortisol promote leptin production in cultured human fat cells. Diabetes 45, 1435–1438.

WO/2002/097036 (S.H. Adams, Inventor), 2002. Compositions and methods for Adipose Abundant Protein. International Patent Application, World Intellectual Property Organization (WIPO).

Wu, Z., Puigserver, P., Andersson, U., Zhang, C., Adelmant, G., Mootha, V., Troy, A., Cinti, S., Lowell, B., Scarpulla, R.C., Spiegelman, B.M., 1999. Mechanisms controlling mitochondrial biogenesis and respiration through the thermogenic coactivator PGC-1. Cell 98, 115–124.

Wu, Z., Xie, Y., Morrison, R.F., Bucher, N.L., Farmer, S.R., 1998. PPARgamma induces the insulin-dependent glucose transporter GLUT4 in the absence of C/EBPalpha during the conversion of 3T3 fibroblasts into adipocytes. J. Clin. Invest. 101, 22–32.

Yu, X.X., Lewin, D.A., Forrest, W., Adams, S.H., 2002. Cold elicits the simultaneous induction of fatty acid synthesis and beta-oxidation in murine brown adipose tissue: prediction from differential gene expression and confirmation in vivo. FASEB J. 16, 155–168.

Yu, X.X., Lewin, D.A., Zhong, A., Brush, J., Schow, P.W., Sherwood, S.W., Pan, G., Adams, S.H., 2001. Overexpression of the human 2-oxoglutarate carrier lowers mitochondrial membrane potential in HEK-293 cells: contrast with the unique cold-induced mitochondrial carrier CGI-69. Biochem. J. 353, 369–375.

Zhou, Y., Sun, X., Jin, L., Stringfield, T., Lin, L., Chen, Y., 2005. Expression profiles of adiponectin receptors in mouse embryos. Gene Expr. Patterns 5, 711–715.